Compressive Deformation of Rohacell Foams: Effects of Strain Rate and Temperature

S. Arezoo[a], V.L. Tagarielli[b,*], C.R. Siviour[a] and N. Petrinic[a]

(a) University of Oxford, Engineering Department, Oxford, OX1 3PJ, UK
(b) Imperial College London, Department of Aeronautics, London, SW7 2AZ, UK

Abstract

Uniaxial compression experiments have been performed on four different densities of Rohacell foam. The experiments explored the sensitivity of the response to the imposed strain rate (in the range $10^{-3} - 5\text{x}10^{3}\ \text{s}^{-1}$) and temperature (203 – 473 K). The compressive collapse stress is generally found to increase with increasing strain rate and decreasing temperature; however this tendency is inverted at very low temperatures or very high strain rates. This behaviour is mainly due to embrittlement of the parent polymer but is also related to the details of the foams' microstructures. Time-temperature superposition is employed to map the temperature sensitivity of the foams to their strain rate dependence. A simple design formula is provided to predict the foam stiffness as a function of temperature and relative density.

Keywords: *Rohacell; polymer foam; strain rate; temperature;*

Submitted to *International Journal of Impact Engineering*, March 2012

[*] Corresponding author. E-mail: v.tagarielli@imperial.ac.uk

1 INTRODUCTION

In the aerospace industry conventional metallic components are increasingly being replaced by composite sandwich structures in an attempt to increase specific stiffness and strength, as well as durability; polymer foams are often used as the core of these sandwich structures. Considering the wide range of temperatures at which structural components in an aircraft operate, and as many components are exposed to the risk of impact loading, it is necessary to develop a thorough understanding of the mechanical response of cellular polymers and their sensitivity to both temperature and applied strain rates.

The uniaxial compressive behaviour of polymer foams as a function of strain rate has been studied by a large number of researchers. Examples include PVC foam [1–3], polystyrene foam [4] epoxy-based and syntactic foams [5–7]. It is generally understood that the stiffness, failure strength, plateau stress and energy absorption of polymer foams show mild strain rate dependency in the quasi-static regime (i.e. for strain rates from 10^{-4} to 1 s^{-1}) and a greater rate sensitivity at high strain rates above 100 s^{-1}; in addition, failure strain decreases with increasing imposed strain rate. The strain rate sensitivity of polymer foams is generally attributed to the inherent viscous elasto-plastic response of the polymeric parent material [8], but it also depends on the foam microstructure [9].

Polymethacrylimide (PMI) foams, commercially known as Rohacell [10], are closed-cell cellular solids, widely used in sandwich applications, where the parent polymer of the cell walls has a density of 1416 kgm^{-3}. The response of these foams is well understood at low strain rates. Zenkert et al [11,12] investigated the macroscopic quasi-static response of Rohacell foams by conducting compression, tension and shear experiments. Other authors have focused on the material response at microscopic length-scales, performing in-situ compression and tension experiments in electron microscopes and deducing the effects of different micro-mechanical mechanisms upon the macroscopic elasto-plastic foam response, as well as the sensitivity of this response to the geometrical features of the microstructure [13]. Some researchers have investigated the strain rate sensitivity of Rohacell foams up to rates of the order of 100 s^{-1} [14,15]. This research focused on the lightest density of Rohacell (51 kg m^{-3})

and concluded that the response was scarcely sensitive to strain rate in the region of $10^{-3} - 10^{2}$ s^{-1}.

While some authors have investigated the response of Rohacell at high temperatures of around 450 K [10], no studies have explored the low temperature behaviour. It is widely observed that stiffness and strength of polymers and polymer foams increase with decreasing temperature [8,16-21], and that embrittlement can affect polymers when the operational temperature falls below a certain threshold [22].

This paper presents a comprehensive experimental study exploring the sensitivity of the compressive elasto-plastic response of a number of commercially available Rohacell foams to both imposed strain rate (in the range 10^{-3} to 5000 s^{-1}, at temperature 296 K) and temperature (in the range 203 to 473 K, at a strain rate 10^{-2} s^{-1}). The similarity between the effects of increasing strain rate and decreasing temperature on the foam response is demonstrated, and a quantitative correspondence between these effects is established by the time-temperature superposition method.

2 Materials and methods

2.1 Materials

Rohacell foams are made from a copolymer of methacrylonitrile (C_4H_5N) and methacrylic acid ($C_4H_6O_2$), with a few key additives including alcohol as a foaming agent. During the foaming process, the liquid copolymer is solidified and Rohacell is produced by thermal expansion of the copolymer sheet in large ovens at high temperatures.

The material examined in this study was obtained in the form of large plates of thickness 50 mm and four different relative densities: 0.04, 0.05, 0.08 and 0.14 ± 2%; these four materials will be denoted by A, B, C and D, respectively. The relative density of each foam was calculated as the ratio of the measured foam density to the density of the parent polymer.

2.2 Specimen Preparation

Circular cylindrical specimens of diameter 9 mm and height of 4 mm were used in tests performed at room temperature, independent of the imposed strain rate. The choice of such small specimens was dictated by the specific requirements of high strain rate testing, namely: rapidly achieving stress equilibrium; minimising stresses due to lateral inertia; and achieving sufficiently high specimen strain rates without yielding the loading bars in the Split-Hopkinson bar used for the experiments. More information about experimental apparatus can be found below. Preliminary quasi-static experiments at room temperature were conducted on specimens of different shape and size (ranging from cylinders of diameter 9 mm and height 4 mm to prismatic cuboidal specimens measuring $30 \times 30 \times 15$ mm) and the measured response was found to be insensitive to specimen shape and size. Quasi-static experiments conducted at different temperatures were performed on cuboidal specimens measuring $15 \times 15 \times 10$ mm; this choice was dictated by the constraints imposed by the environmental chamber used in the tests. All samples were machined by conventional methods and were cut in such a way that the specimen's axis was aligned with the thickness direction of the foam plates.

2.3 Quasi-static and medium rate experiments

Uniaxial compression experiments were performed at room temperature and at different strain rates in order to determine the sensitivity of the mechanical response to the loading rate. Strain rates between 10^{-3} and 0.1 s^{-1} were achieved using a screw-driven tensometer which forced plastic collapse of the specimen by means of two flat metal platens whose surface was lubricated with PTFE spray. The load was measured with a resistive load cell whereas compressive strains were measured by a non-contact laser extensometer of resolution 1μm ; tests were also video-recorded by a digital camera in order to observe the macroscopic mechanism of deformation.

Medium strain rates (1 to 100 s^{-1}) were achieved using a bespoke, hydraulically-driven loading rig fitted with a resistive dynamic load cell. The specimen was placed in contact with two lightweight metallic cylinders; one of these cylinders was stationary while the other one was accelerated to speeds of the order of 2 m s^{-1} (with negligible acceleration times), causing plastic deformation of the specimen. The shortening of the specimen was measured by a high speed video-camera (Vision Research, Phantom model 7.1) and

bespoke image analysis software, thereby determining the strain history for the specimen.

2.4 SHPB experiments

High strain rates (ranging from 800 to 5000 s^{-1}) were obtained with a split-Hopkinson pressure bar setup (SHPB). A detailed description of this test method is provided in [23]. Due to the low strength of the polymer foams tested in this study, a dedicated Hopkinson bar of enhanced sensitivity was developed in order to increase the signal-to-noise ratio [23–25]. The apparatus was similar to that developed by other authors for materials of similar strength [3] and comprised magnesium alloy bars of diameter 12.7 mm, the input and output bars were 1 m and 0.5 m long respectively. Both bars were instrumented with foil strain gauge stations placed halfway along the length of the input bar and at a distance of 50 mm from the specimen end of the output bar. Forces in the bar were recorded by connecting the strain gauge stations to a Wheatstone bridge and a 500 kHz Fylde signal amplifier with a gain of 1000. The gauges were calibrated statically and dynamically. The displacement of the specimen ends were obtained by both direct observation using an ultra-high speed camera (model SIM-X 16) and calculation via the classic analysis of the force signals; the two methods provided similar strain-time histories.

High-speed photographs were used to measure the history of strain field in the specimen as a function of time, by means of a digital image correlation procedure; it was found that the strain field in the specimens was uniform. It was also observed that while foams A, B and C showed a ductile response, with little evidence of fracture, foam D underwent brittle microcracking upon compression; the material in contact with the input bar was progressively eroded with increasing applied strain, and this manifested in a uniform cloud of sub-mm fragments being ejected radially during the test.

Stress versus strain histories measured with the SHPB setup are only valid after dynamic stress equilibrium of the specimen has been achieved, i.e., when the forces exerted on the sample by the input and output bars attain the same value. For each of the experiments performed the instant at which equilibrium was achieved was determined, by plotting the forces in the input and output bar as functions of time; Fig. 1 gives an

example of such plots for foam D tested at a strain rate of 1500 s^{-1}. It is clear that the specimen is in equilibrium after about $50\,\mu s$ from the beginning of the test; at this time the compressive strain in the specimen is of the order of 0.1, i.e., the applied strain is in excess of the yield strain. A similar response was observed for all SHPB experiments. It follows that the SHPB experiments cannot be used to calculate the apparent stiffness of the material; on the other hand, they permit valid measurements of the flow stress of the foam during the plastic collapse phase.

2.5 Compression tests at different temperatures

Quasi-static compression experiments were conducted on the cuboidal specimens described above at a nominal imposed strain rate of 0.01 s^{-1} and at seven temperatures (namely, 203, 233, 263, 278, 296, 343 and 473 K) in order to determine the sensitivity of the response of all foams to temperature. The tests were performed in a screw-driven Instron machine coupled with an environmental chamber; load was measured by a resistive load cell of 5 kN capacity placed outside the chamber, while specimen shortening was measured by a mechanical, resistive extensometer connected to the loading platens (after calibration of this extensometer at all the temperatures at which tests were performed). The chamber was equipped with resistive heating elements which were employed in tests above room temperature; low temperatures were obtained by circulation of cold nitrogen vapour inside the chamber, and the temperature control was performed automatically by the environmental chamber: an additional temperature reading was obtained by a thermocouple connected to the loading platens. In all tests the platens were lubricated with petroleum jelly [26] in order to minimise friction. The material stiffness was measured by conducting selected quasi-static experiments where the specimen was unloaded after compressive deformation to strains of the order of 5%; the stiffness was defined as the initial slope of the unloading part of the stress-strain response.

3 Results and discussion

3.1 Strain rate sensitivity of the response at room temperature

Preliminary quasi-static compression experiments conducted on all foam densities, with specimens cut in three mutually perpendicular directions, confirmed that the material response was insensitive to direction. Compressive tests at all strain rates were repeated a minimum of five times and it was found that the measured stress versus strain response was highly repeatable, with scatter in flow stress below 10%.

Selected compressive stress versus strain responses for all four foam densities are shown in Fig. 2, which includes data from low, medium and high strain rate tests for foams A, B, C and D. The different foams display different sensitivity to the imposed strain rate. Foams A and B exhibit a mild rate sensitivity, with the plateau stress increasing by around 20 to 30% when the strain rate is increased from $10^{-3}\,s^{-1}$ to $10^{3}\,s^{-1}$. Foam C exhibits an almost rate insensitive behaviour; in contrast, the flow stress of foam D increases by more than 30% with strain rate increasing from $10^{-3}\,s^{-1}$ to $10^{2}\,s^{-1}$, but then decreases as the applied strain rate reaches $10^{3}\,s^{-1}$. For all foams and at all strain rates, negligible transverse strain was observed in the photographs taken during the experiments, implying that for these foams the plastic Poisson's ratio is close to zero.

At strain rates up to $10^{2}\,s^{-1}$ the response of all foams comprises a linear phase followed by plastic collapse at negligible strain-hardening (plateau phase) and final densification. At higher strain rates, on the order of $10^{3}\,s^{-1}$, the stress/strain curves for all foams display higher oscillations in stress, indicating a more brittle response. The plastic collapse response of the material is different in the four foams tested at high strain rate; while foams A and B display a mild strain hardening response, C collapses at approximately constant flow stress, whereas D exhibits a mild strain softening. The softening of D is in line with the brittle fracture mechanism observed via high-speed photography at high strain rates (Section 2.4). Densification cannot be observed in the SHPB tests, in which the loading ends at compressive strains of the order of 0.5.

In order to summarise the strain rate dependence of the four foams tested, Fig. 3 shows the measured collapse stress (defined as the flow stress at a nominal plastic strain of 0.2) as a function of the applied strain rate for all specimens; similar trends are followed by

the plateau stress (defined as the average flow stress at nominal compressive strains between 0.1 and 0.5) versus strain rate data. The low strength of D at high strain rates is again consistent with the brittle failure mechanisms displayed in SHPB tests for this foam. Embrittlement of polymers at high rates of strain is commonly observed [27–29], and different authors have reported a similar behaviour for other polymeric foams (e.g. [6]). However, embrittlement of the parent polymer is not necessarily the only reason for the brittle response of D at high strain rates, given the different response observed in other foams made from the same polymer at the same strain rates. It was reported in [13] that the four foams under investigation possess different microstructural features, such as cell size and wall thickness. Note that the local maximum strain in the cell walls scales linearly with the microscopically applied strain rate [8] by a constant of proportionality which depends on the geometrical details of the microstructure (assuming microscopic collapse by plastic cell wall bending); it is therefore possible that the relatively long and slender cell walls of foams of low density result in lower local strain rates than those applied to the stockier cell walls of D, for a given imposed macroscopic strain rate. In addition, upon compression, the gas trapped in these closed cell foams can affect the state of stress at a microscopic level and therefore the onset of failure. However, a detailed analysis of the relative influence of these mechanisms upon the macroscopic foam response is beyond the scope of this study.

3.2 Sensitivity of the quasi-static response to temperature

Figure 4 presents a summary of the measured compressive stress-strain response for all foams at a strain rate of $10^{-2}\,s^{-1}$ and at temperatures ranging from 203 to 473 K. At the highest temperature of 473 K, all foams display a rubbery response with no clearly defined yield point, indicating that the material is above its glass transition temperature and undergoes viscous flow; Fig. 5 contains photographs of specimens made from all foam materials after testing at this temperature, and shows that foams underwent permanent deformation, driven by the trapped gas in the foams' closed cells. The lateral 'bulging' of the specimens is more pronounced for foam D. Fig. 6a shows the sensitivity of the measured foam stiffness to temperature; it is clear that the stiffness of all foams has dropped substantially at 473 K, consistent with them being above their glass transition temperature.

If the temperature is decreased to the range 233-343 K, the measured response of all foams shows an approximately linear viscoelastic phase followed by visco-plastic collapse and final densification, with stiffness increasing with decreasing temperature, as shown in Fig. 6a. At the lowest temperature of this range (233 K) the measured flow stress begins displaying oscillations, indicating a transition towards a brittle response.

When the temperature is further decreased to 203 K all foams display high oscillations in the measured stress/strain history, clearly indicating a brittle response (a further indication of a brittle response was the high level of acoustic emission observed for tests at this temperature). Foams of different densities show a different hardening response at 203 K: while A collapses at a constant stress prior to densification, B and C display an initial strain hardening and subsequent strain softening, attributable to fracture events, prior to densification. The D foam shows an approximately linear strain softening after the onset of collapse. Evidence of brittle response at 203 K can be gathered by observing different foam specimens following the compression experiments, as shown in the lower part of Fig. 5; it is also clear from these photographs that foams of lower relative density show less evidence of fracture mechanisms while foams of higher density, such as D, display a pronounced brittle response with evident cracking.

Figure 6b presents the sensitivity of the collapse stress (again, defined as the flow stress at a nominal plastic strain of 0.2) to temperature (similar trends are observed for the plateau stress). As the temperature is decreased from 473 K the collapse stress tends to increase; however at a critical temperature this tendency is inverted and the collapse stress decreases by further decreasing the temperature. The critical temperatures are approximately 203 K, 263 K, 278 K and 263 K for foams D, C, B and A, respectively. The measured sensitivity of the collapse stress to increasing imposed strain rate (Figs. 2, 3) is remarkably similar to the sensitivity exhibited by the foams to decreasing temperature (Figs. 4, 6b). Fig. 7 shows a direct comparison of selected stress/strain histories: in figure 7a the similarity of the high strain rate response of D at room temperature and the quasi-static response of the same foam at 203 K is outlined; in figure 7b it is shown that for the case of foam A, the quasi-static response at 203 K is more similar to the medium-rate response at room temperature than to the high strain rate response at room temperature; however it should be noted that the quasi-static

collapse stress at 203 K is only 15% lower than the collapse stress at room temperature and high strain rate.

The observations above reinforce the idea that the sensitivity of the response of these foams to temperature and strain rate is mainly related to the strain rate and temperature sensitivity of the parent polymer, with the details of the foams microstructure having a less important effect. If this is the case, the time-temperature superposition principle can be employed to map the data obtained at different strain rates to the data measured at different temperatures; this is shown in Fig. 8, where the mapping has been performed, for the measured collapse stress, by the empirical formula [30,31]

$$T = T_0 + A(\log \dot{\varepsilon}_0 - \log \dot{\varepsilon}) \tag{1}$$

where T_0 is a reference temperature (room temperature of 296 K), $\dot{\varepsilon}_0 = 10^{-2}\,\mathrm{s}^{-1}$ is a reference strain rate and A is a mapping parameter which was taken as 17 K per decade of strain rate. The mapping is accurate within 10-15% in the range 203 to 296 K which corresponds, by the mapping provided by eq. (1), to strain rates in the range $10^{-2} - 3\cdot 10^{3}\,\mathrm{s}^{-1}$.

3.3 Foam stiffness

Arezoo et al [13] measured the sensitivity of the apparent compressive foam stiffness E_F to the relative density $\overline{\rho}$ at $\dot{\varepsilon} = 10^{-2}\,\mathrm{s}^{-1}$ and $T = 296\,\mathrm{K}$ and found that this could be expressed by the power-law relation $E_F = E_S\,\overline{\rho}^{\,m_E}$ where $E_S = 4106\,\mathrm{MPa}$ is the compressive stiffness of the solid parent polymer material at the same strain rate and temperature, and $m_E = 1.47$ is a material property. It is known that at temperatures well below the glass transition temperature T_g the stiffness of solid polymers can be taken to vary linearly with temperature

$$E_S(T) = E_S^0\left(1 - \alpha\frac{T}{T_g}\right) = E_S^0(1 - \beta T) \tag{2}$$

where E_S^0 is the stiffness of the polymer at 0 K and β is a fit parameter. Upon assuming that the scaling relation measured by [13] is valid at every temperature, we can write

$$E_F / \overline{\rho}^{\,m_E} = E_S^0(1 - \beta T) \tag{3}$$

which gives the foam stiffness as a function of relative density and temperature. Figure 9 shows a best fit of eq. (3) through the measurements conducted in this study, giving $E_S^0 = 10125\,\text{MPa}$ and $\beta = 2.14 \cdot 10^{-3}\,\text{K}^{-1}$ for the Rohacell foams investigated here. This formula can be employed to obtain estimates of foam stiffness in preliminary design calculations.

4 CONCLUSIONS

The uniaxial compressive response of Rohacell foams of various densities was measured at strain rates from 10^{-3} to $5 \cdot 10^{3}\,\text{s}^{-1}$ and at temperatures ranging from 203 to 473 K. All foams exhibited mild strain rate sensitivity and a ductile response at low to medium strain rates, but showed progressive embrittlement as the strain rates were increased beyond $100\,\text{s}^{-1}$. The materials displayed great sensitivity to the imposed temperature; the response was of rubbery type at 473 K, but showed the characteristics of an elasto-plastic compressible solid in the range 233-343 K. At the lowest temperature (203 K) all foams showed an elastic-brittle response, however the tendency towards a brittle response was more pronounced for foams of higher relative density.

Observations suggest that the sensitivity of the foams response to strain rate and temperature is principally governed by the inherent sensitivity of the parent polymer blend, with a minor effect of microstructural features and micro-inertia. The time-temperature superposition allowed mapping of the strain rate sensitivity of the foams to the sensitivity of the response at different temperatures. A simple formula was also provided to give initial estimates of the foam stiffness as a function of temperature and relative density.

ACKNOWLEDGEMENTS

The authors would like to thank Röhm Ltd (Germany) for providing the Rohacell foam material and acknowledge the assistance of Dr Igor Dyson with experiments. Sara Arezoo acknowledges the financial support of Rolls-Royce plc (Dr Julian Reed) for a DPhil course at the University of Oxford.

References

[1] T. Thomas, H. Mahfuz, L. a Carlsson, K. Kanny, S. Jeelani, Composite Structures 58 (2002) 505-512.

[2] T. Thomas, H. Mahfuz, K. Kanny, S. Jeelani, Journal of Reinforced Plastics and Composites 23 (2004) 739-749.

[3] V.L. Tagarielli, V.S. Deshpande, N.A. Fleck, Composites Part B: Engineering 39 (2008) 83-91.

[4] B. Song, International Journal of Impact Engineering 31 (2005) 509-521.

[5] B. Song, W. Chen, W.-Y. Lu, Journal of Materials Science 42 (2007) 7502-7507.

[6] B. Song, W. Chen, D.J. Frew, Journal of Composite Materials 38 (2004) 915-936.

[7] P. Li, N. Petrinic, C.R. Siviour, R. Froud, J.M. Reed, Materials Science and Engineering: A 515 (2009) 19-25.

[8] L.J. Gibson, M.F. Ashby, Cellular Solids Structures and Properties - Second Edition, Cambridge, 1999.

[9] S.R. Reid, C. Peng, International Journal of Impact Engineering 19 (1997) 531-570.

[10] Roehm Degussa-Huls group, Www.roehm.com (n.d.).

[11] D. Zenkert, a. Shipsha, M. Burman, Journal of Sandwich Structures and Materials 8 (2006) 517-538.

[12] D. Zenkert, M. Burman, Composites Science and Technology 69 (2009) 785-792.

[13] S. Arezoo, V.L. Tagarielli, N. Petrinic, J.M. Reed, Journal of Materials Science 46 (2011) 6863-6870.

[14] Q. Li, International Journal of Solids and Structures 37 (2000) 6321-6341.

[15] R. a. W. Mines, Applied Mechanics and Materials 7-8 (2007) 231-236.

[16] B.Z. Jang, D.R. Uhlmann, J.B.V. Sande, Journal of Applied Polymer Science 29 (1984) 3409-3420.

[17] J. Richeton, S. Ahzi, K. Vecchio, F. Jiang, R. Adharapurapu, International Journal of Solids and Structures 43 (2006) 2318-2335.

[18] B. Song, Composite Structures 67 (2005) 289-298.

[19] B. Song, W.-Y. Lu, W. Chen, DYMAT 2009 - 9th International Conferences on the Mechanical and Physical Behaviour of Materials Under Dynamic Loading 2 (2009) 1251-1256.

[20] B. Song, W.-yang Lu, W. Chen, S.N. Laboratories, Experimental Mechanics (2009).

[21] B. Song, W.-Y. Lu, C.J. Syn, W. Chen, Journal of Materials Science 44 (2008) 351-357.

[22] S.M. Soni, R.F. Gibson, E.O. Ayorinde, Composites Science and Technology 69 (2009) 829-838.

[23] G.T. Gray III, Classic Split-Hopkinson Pressure Bar Technique ASM V8 Mechanical Testing, 1999.

[24] W. Chen, F. Lu, D.J. Frew, M.J. Forrestal, Journal of Applied Mechanics 69 (2002) 214.

[25] W. Chen, B. Zhang, M.J. Forrestal, Experimental Mechanics 39 (1999) 81-85.

[26] A. Trautmann, C.R. Siviour, S.M. Walley, J.E. Field, International Journal of Impact Engineering 31 (2005) 523-544.

[27] E.M. Arruda, M.C. Boyce, R. Jayachandran, Mechanics of Materials 19 (1995) 193-212.

[28] Mulliken, M. Boyce, International Journal of Solids and Structures 43 (2006) 1331-1356.

[29] J. Richeton, S. Ahzi, K. Vecchio, F. Jiang, R. Adharapurapu, International Journal of Solids and Structures 43 (2006) 2318-2335.

[30] D.M. Williamson, C.R. Siviour, W.G. Proud, S.J.P. Palmer, R. Govier, K. Ellis, P. Blackwell and C. Leppard (2008). Temperature-time response of a polymer bonded explosive in compression (EDC37), J. Phys. D: Appl. Phys. 41, 085404.

[31] C.R. Siviour, S.M. Walley, W.G. Proud and J.E. Field (2005). The high strain rate compressive behaviour of polycarbonate and polyvinylidene difluoride. Polymer, 46**,** 12546-12555.

Figure captions

Fig. 1. Time histories of the compressive forces applied at the specimen ends by the input and output bars; equilibrium is achieved after approximately $50\ \mu s$.

Fig. 2. Compressive stress-strain response of Rohacell foams at different strain rates.

Fig. 3. Summary of the sensitivity of the compressive collapse stress to the imposed strain rate, for all the foams tested in this study.

Fig. 1. Compressive stress-strain response of Rohacell foams at different temperatures in the range 203-473.

Fig. 2. Photographs of foam specimens after quasi-static compression (up to densification strain) at temperatures of 203 and 473 K.

Fig. 6. Summary of the sensitivity of (a) the foam stiffness and (b) the collapse stress to temperature, for all foams tested in this study.

Fig. 7. (a) Comparison of two stress/strain responses of R200 at $\left(\dot{\varepsilon} = 10^{3}\,\mathrm{s}^{-1},\ T = 298\,\mathrm{K}\right)$ and $\left(\dot{\varepsilon} = 10^{-3}\,\mathrm{s}^{-1},\ T = 203\,\mathrm{K}\right)$; (b) comparison of three stress/strain responses of R51, namely: $\left(\dot{\varepsilon} = 10^{3}\,\mathrm{s}^{-1},\ T = 298\,\mathrm{K}\right)$, $\left(\dot{\varepsilon} = 10^{-3}\,\mathrm{s}^{-1},\ T = 203\,\mathrm{K}\right)$ and $\left(\dot{\varepsilon} = 10^{2}\,\mathrm{s}^{-1},\ T = 298\,\mathrm{K}\right)$.

Fig. 8. Measured collapse stress as a function of temperature; data obtained at different strain rates was mapped to the temperature axis by using eq. (1).

Fig. 9. Normalised apparent foam stiffness versus temperature. Predictions from eq. (3) are compared to experimental data for all foams tested.

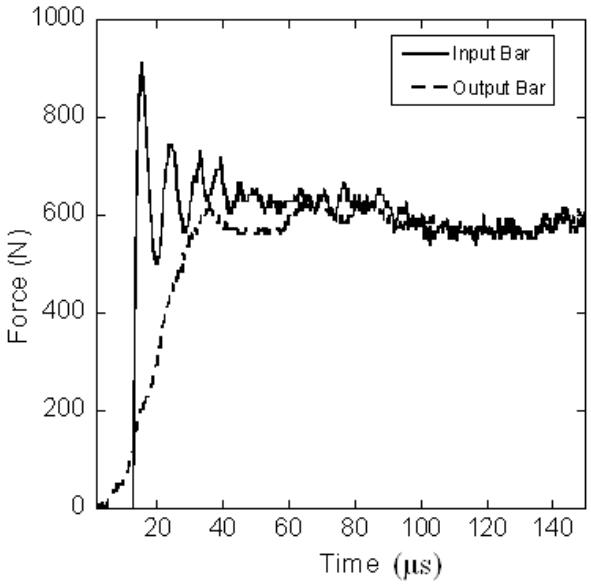

Fig. 1. Time histories of the compressive forces applied at the specimen ends by the input and output bars; equilibrium is achieved after approximately 50 μs.

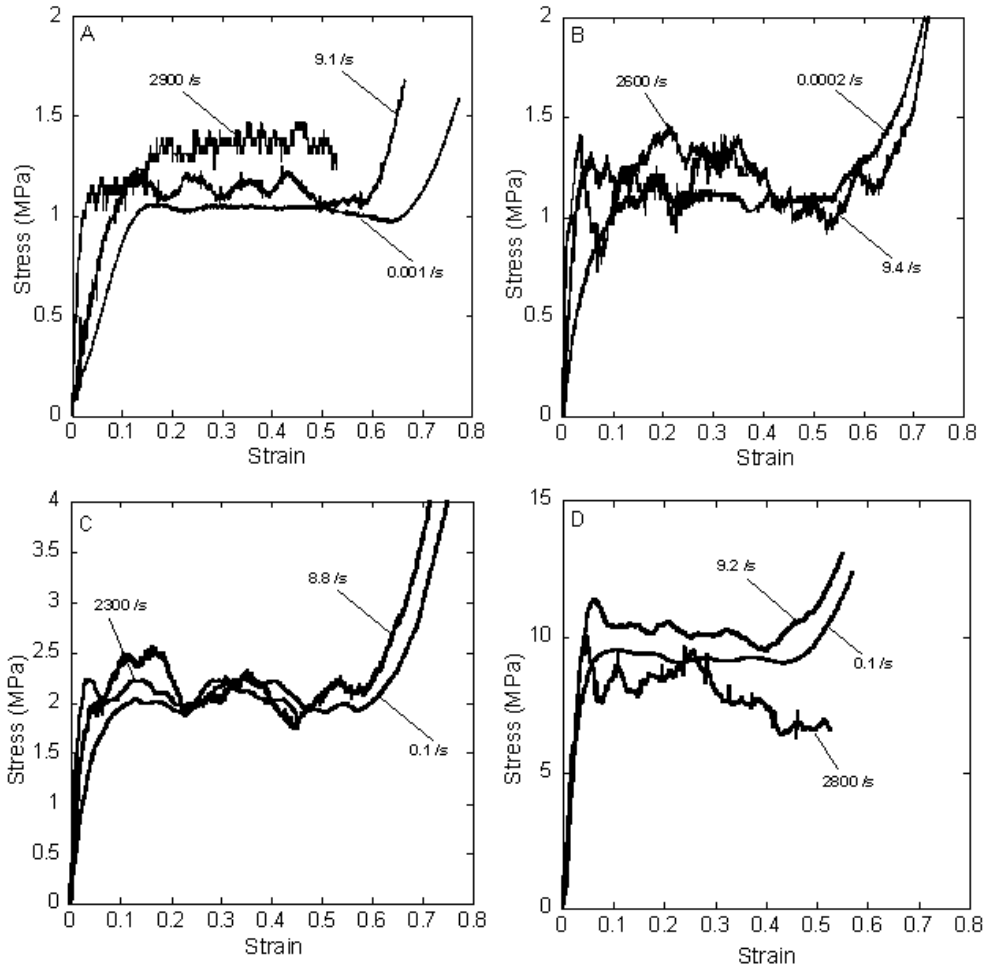

Fig. 2. Compressive stress-strain response of Rohacell foams at room temperature and different strain rates.

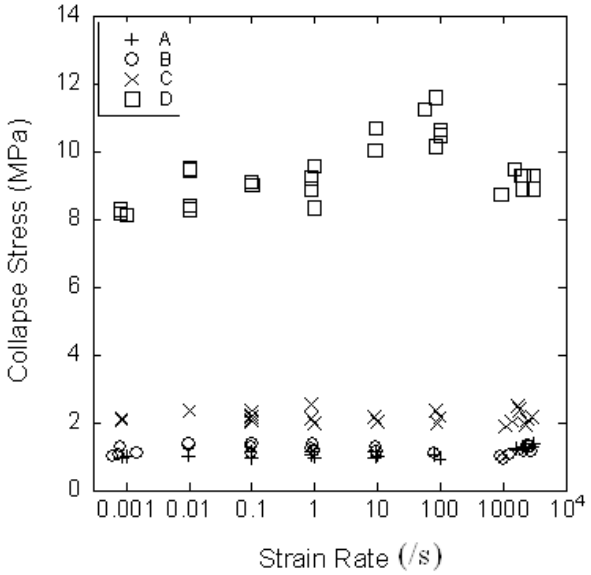

Fig. 3. Summary of the sensitivity of the compressive collapse stress to the imposed strain rate, for all the foams tested in this study.

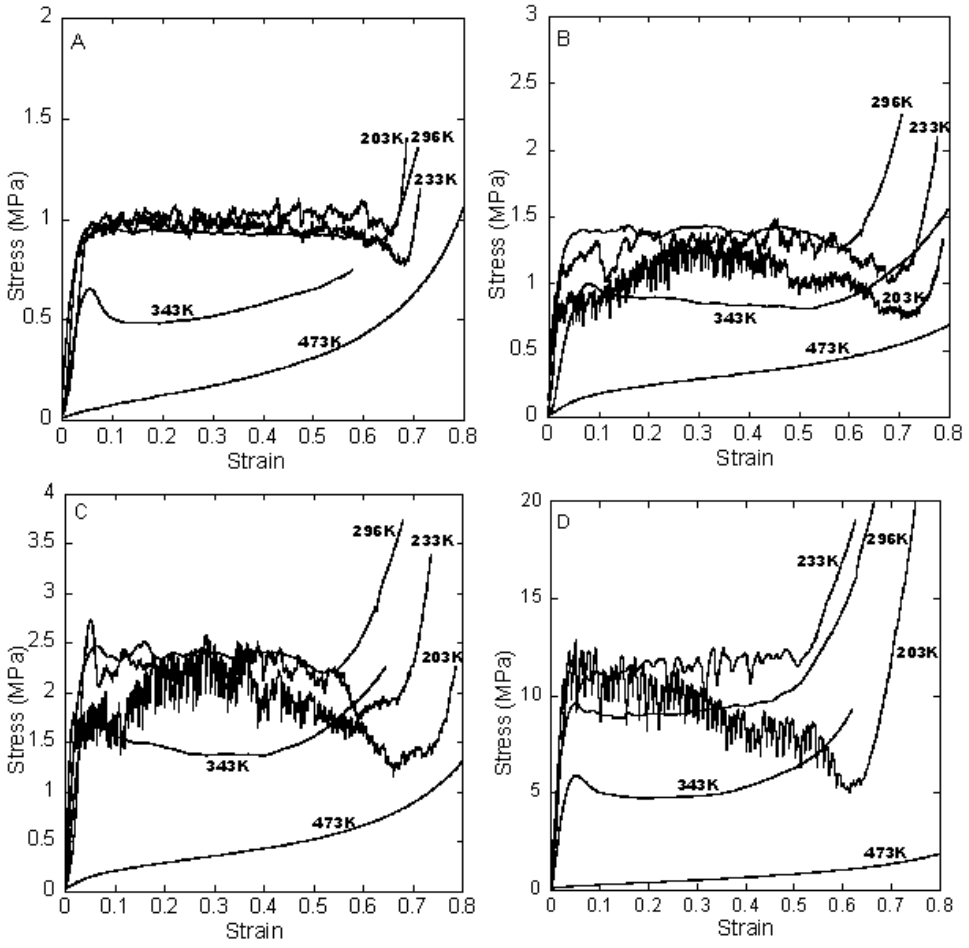

Fig. 4. Compressive stress-strain response of Rohacell foams at different temperatures in the range 203-473 K.

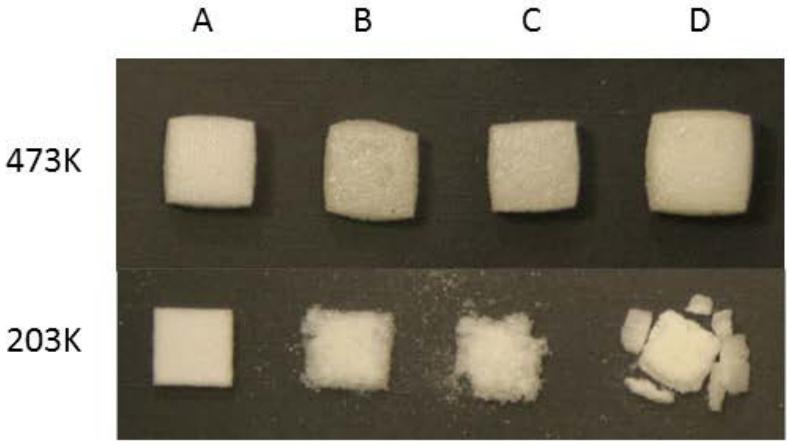

Fig. 5. Photographs of foam specimens after quasi-static compression (up to densification strain) at temperatures of 203 and 473 K.

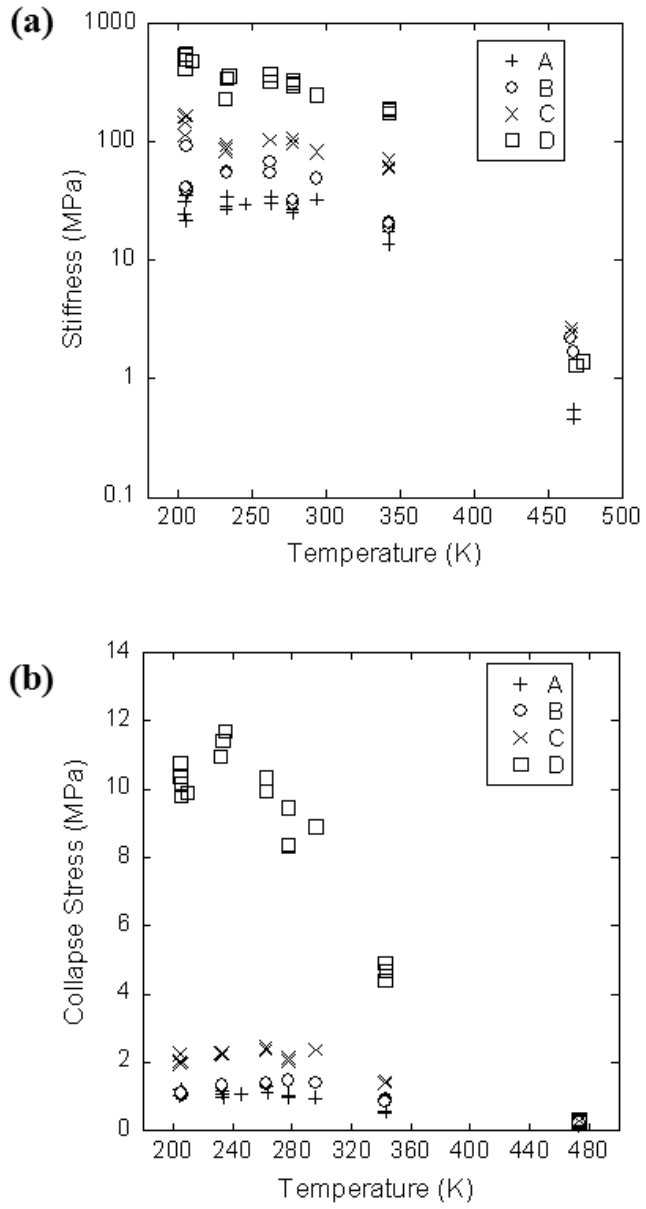

Fig. 6. Summary of the sensitivity of (a) the foam stiffness and (b) the collapse stress to temperature, for all foams tested in this study.

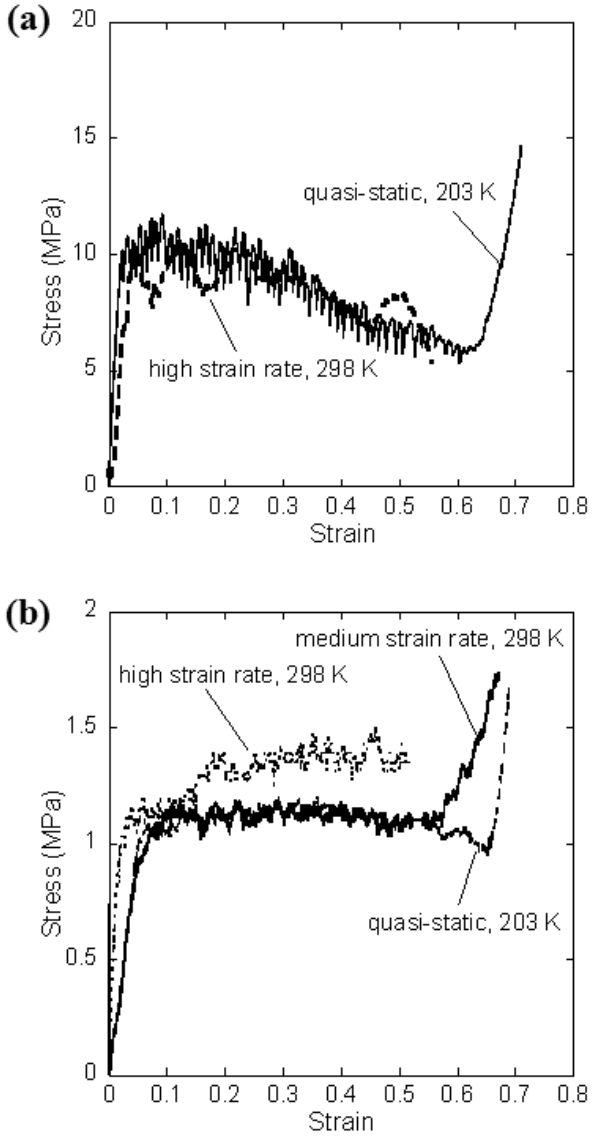

Fig. 7. (a) Comparison of two stress/strain responses of **D** at $\left(\dot{\varepsilon}=10^{3}\,s^{-1},\ T=298\mathrm{K}\right)$ and $\left(\dot{\varepsilon}=10^{-3}\,s^{-1},\ T=203\mathrm{K}\right)$; (b) comparison of three stress/strain responses of **A**, namely: $\left(\dot{\varepsilon}=10^{3}\,s^{-1},\ T=298\mathrm{K}\right)$, $\left(\dot{\varepsilon}=10^{-3}\,s^{-1},\ T=203\mathrm{K}\right)$ and $\left(\dot{\varepsilon}=10^{2}s^{-1},\ T=298\mathrm{K}\right)$.

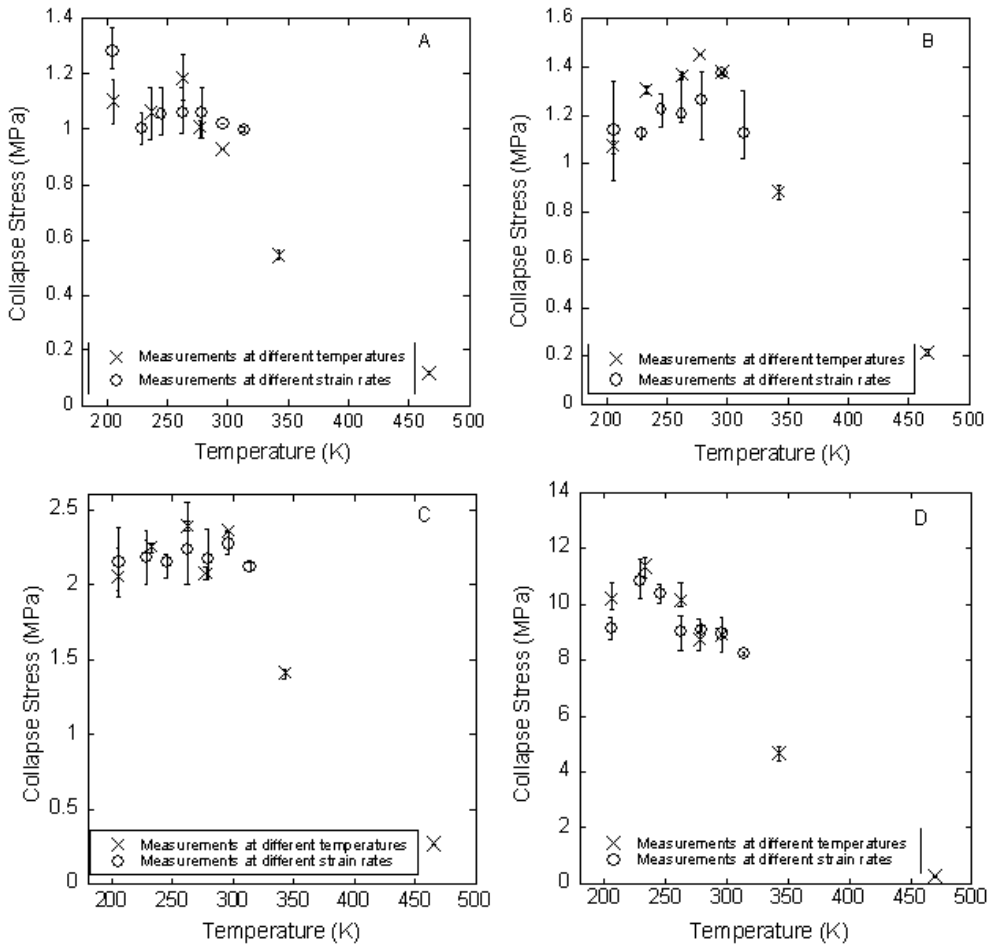

Fig. 8. Measured collapse stress as a function of temperature; data obtained at different strain rates was mapped to the temperature axis by using eq. (1).

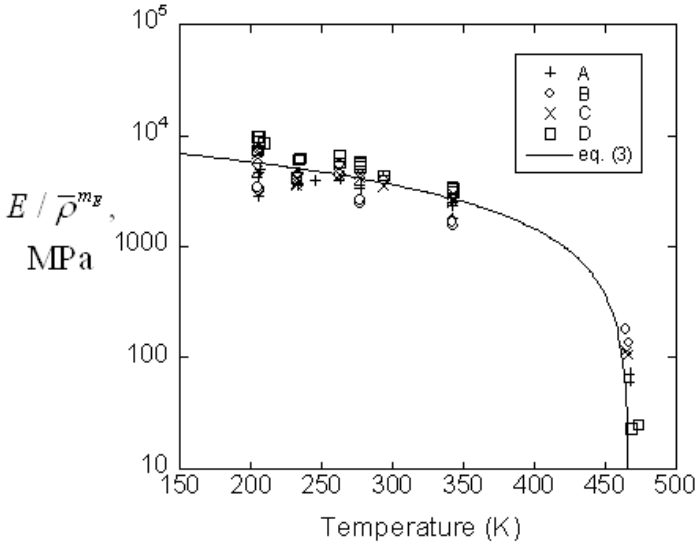

Fig. 9. Normalised apparent foam stiffness versus temperature. Predictions from eq. (3) are compared to experimental data for all foams tested.